Supplementary Information

Dual active sites of single-atom copper and oxygen vacancy formed in-situ on ultrathin TiO_2(B) nanosheet boost the photocatalytic dehalogenative C–C coupling synthesis of bibenzyl

Qifeng Chen[#a*], Peng Zheng[#a], Haodi Liu[a], Yuanrong Zhang[a], Shuaitao Li[a], Hongpian Guo[a], Yanfen Fang[b*], Xun Hu[a*], Ran Duan[c]

[a] Dr. & Prof. Qifeng Chen, MS Peng Zheng, MS Yuanrong Zhang, MS Shuaitao Li, Miss Hongpian Guo, Dr. & Prof. Xun Hu, School of Materials Science & Engineering, University of Jinan, No. 336, West Road of Nan Xinzhuang, Jinan 250022, Shandong, China, *qfchen@126.com* (Qifeng Chen); *mse_hux@ujn.edu.cn* (Xun Hu).

[b] Prof. Yanfen Fang, College of Biological and Pharmaceutical Sciences, China Three Gorges University, Yichang, China, 443002, *fangyf@ctgu.edu.cn*.

[c] Ms Ran Duan, Institute of Chemistry, Chinese Academy of Sciences, Zhongguancun North First Street 2, Beijing, 100190, China.

Photoelectrochemical measurement. In the photocurrent measurement process, we used an Ag/AgCl electrode (3.0 M KCl) as the reference electrode and a platinum electrode as the counter electrode. The working electrode was prepared by impregnating the sample on FTO glass. The measurement of the three-electrode system was carried out in Na_2SO_4 (0.2 M) electrolyte. For the electrochemical impedance test, the three-electrode system was measured in a mixture of 0.1 M potassium ferricyanide and 0.1 M potassium ferrocyanide electrolyte. The measurement frequency of Nyquist plot was 1×10^6 ~ 0.01 Hz.

The working electrode was prepared as follows: 3.0 mg of photocatalysts were added into a mixture of 0.3 mL ethanol and 0.1 mL Nafion (0.1 wt%, Alfar Aesar). A homogeneous suspension was obtained by using ultrasonic oscillation for 10 min. Then, the photocatalyst suspension was dropped onto the FTO glass under an infrared lamp. After solvent volatilization, the working electrode with an active area (covered by photocatalysts) of 1.0 cm^2 was obtained.

Preparation of AFM sample. A specific amount of TiO_2(B) was dispersed in ethanol solution under ultrasonic treatment. Drops of the dispersed liquid were then added drop by drop to the mica sheet. After drying, the sample was photographed with a Bruker Dimension Icon AFM instrument.

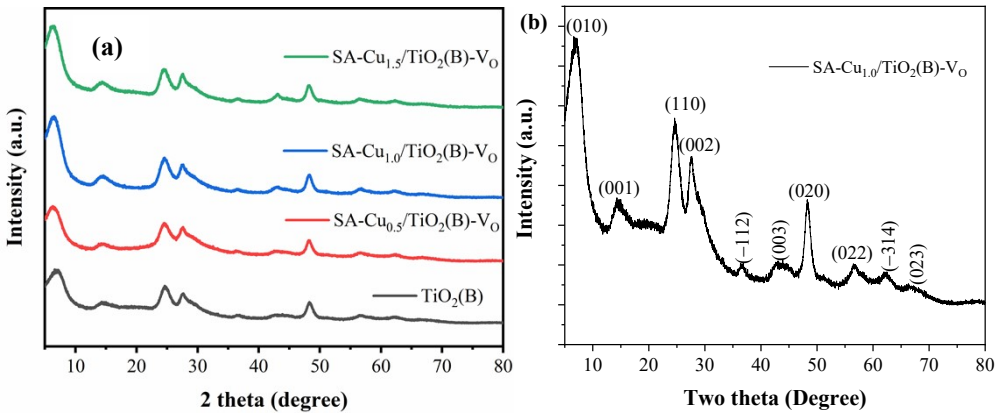

Fig. S1 XRD patterns of SA-Cu_x/TiO_2(B)-V_O photocatalysts (a), and enlarged XRD pattern of SA-$Cu_{1.0}$/TiO_2(B)-V_O.

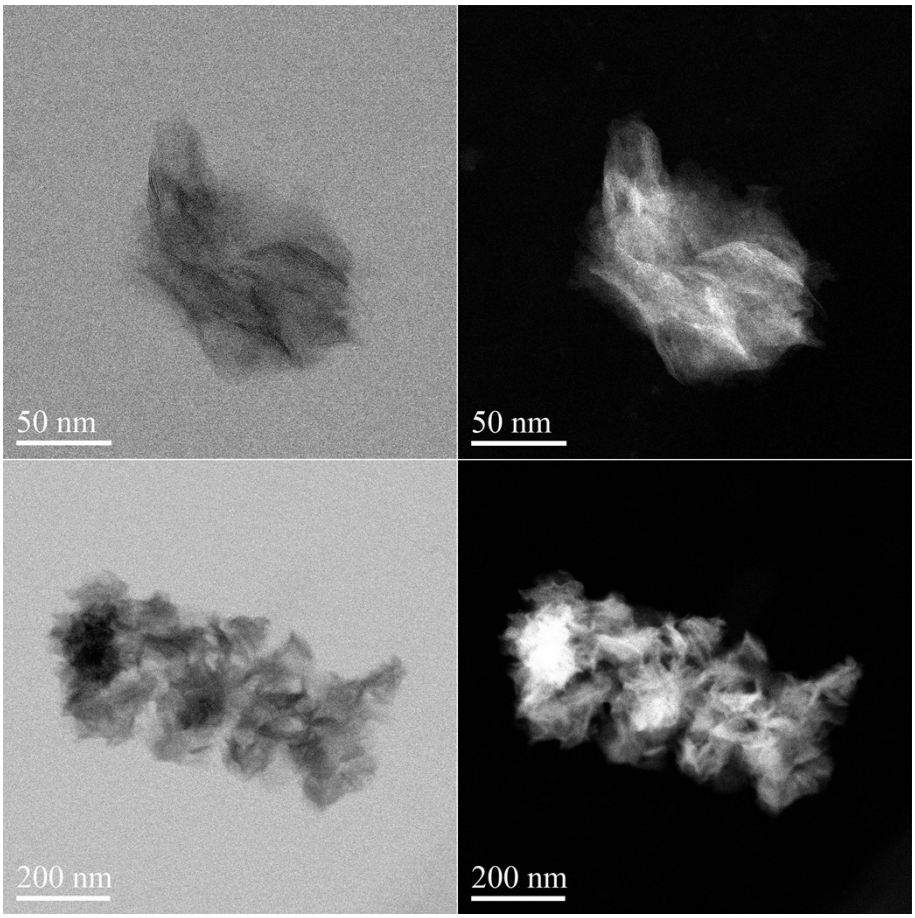

Fig. S2 HAADF-STEM images of SA-$Cu_{1.0}$/TiO_2(B)-V_O.

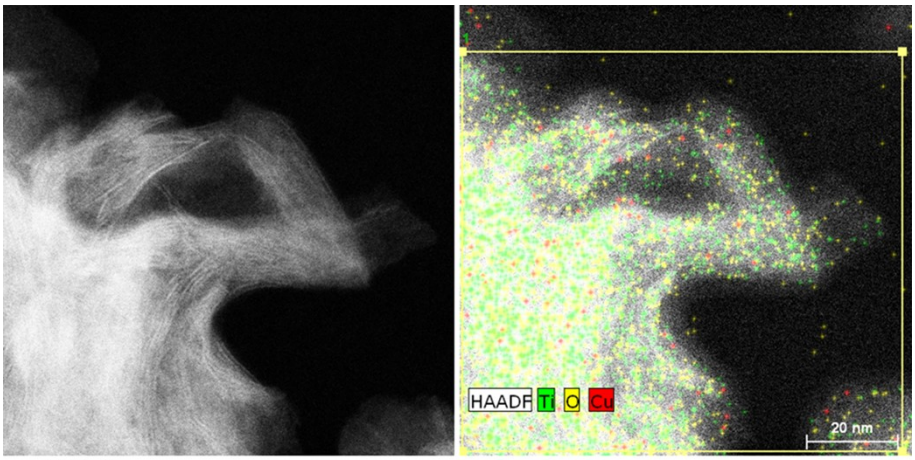

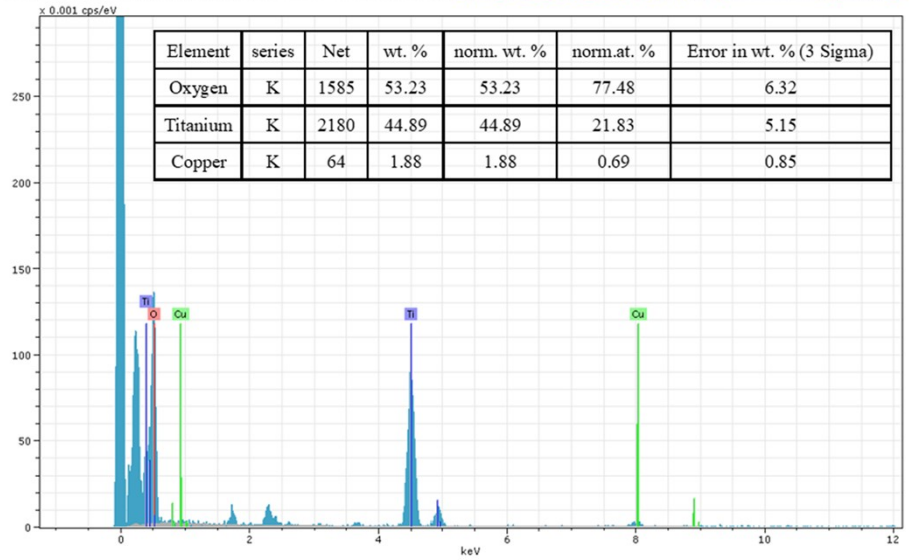

Element	series	Net	wt. %	norm. wt. %	norm.at. %	Error in wt. % (3 Sigma)
Oxygen	K	1585	53.23	53.23	77.48	6.32
Titanium	K	2180	44.89	44.89	21.83	5.15
Copper	K	64	1.88	1.88	0.69	0.85

Fig. S3 EDS spectrum and analysis of SA-$Cu_{1.0}/TiO_2$(B)-V_O.

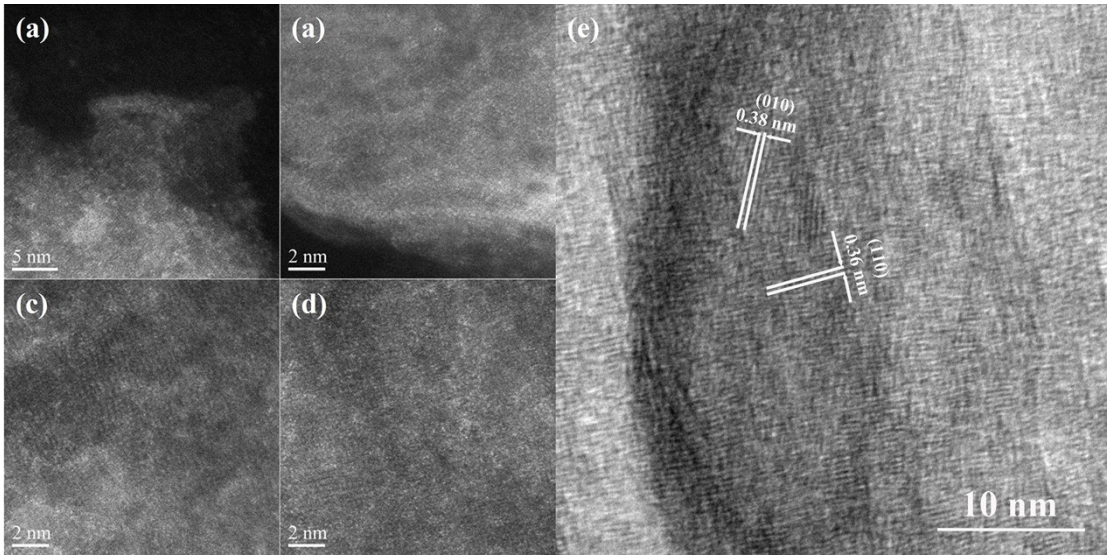

Fig. S4 AC-HAADF-STEM images of SA-Cu/TiO_2(B)-V_O (a-d) and HRTEM image of TiO_2(B) (e).

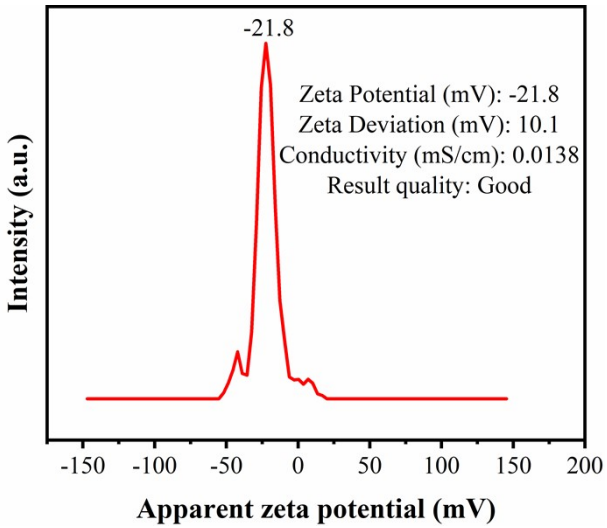

Fig. S5 The result of the Zeta potential test of TiO_2(B). 1.0 mg of the samples were dispersed in 5.0 mL H_2O, and then performed the test.

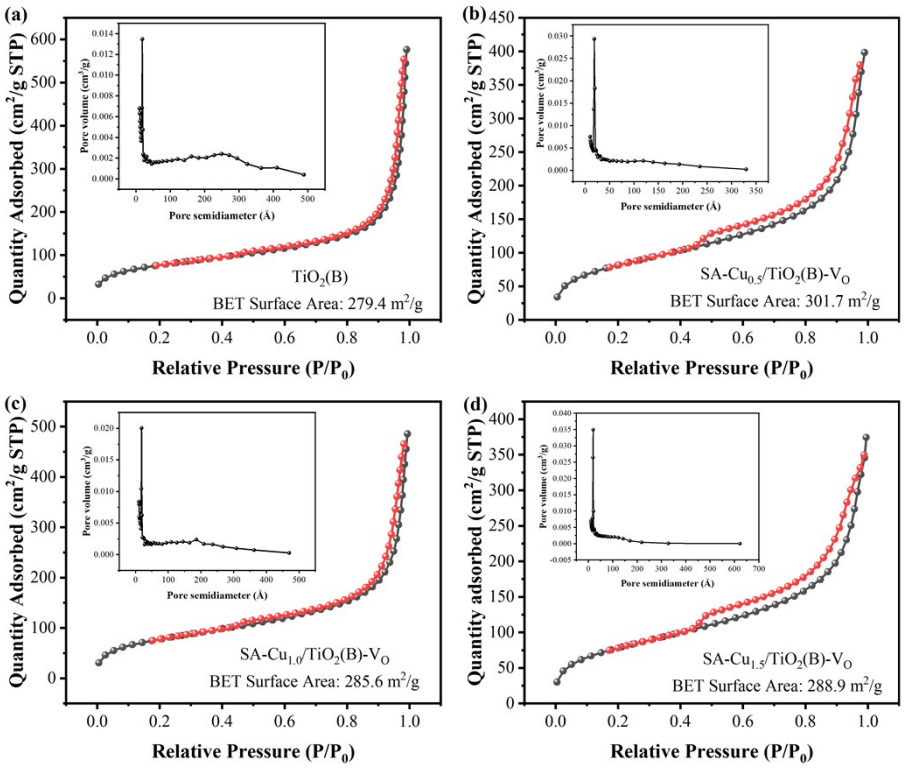

Fig. S6 Nitrogen adsorption/desorption isotherm and pore size distribution of various photocatalysts

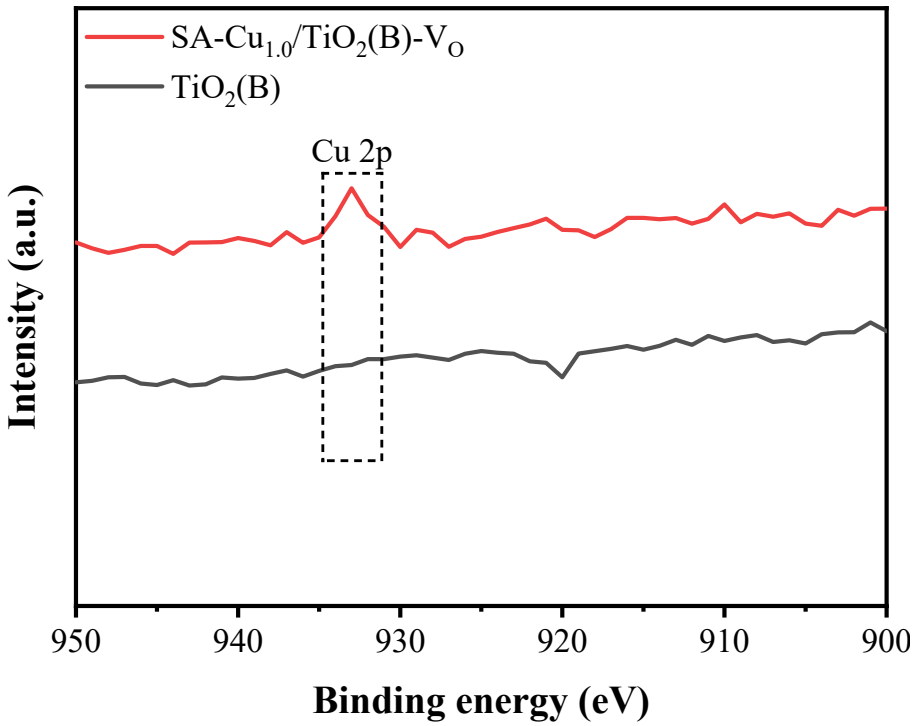

Fig. S7 Partially enlarged XPS survey spectra of TiO_2(B) and SA-$Cu_{1.0}$/TiO_2(B)-VO.

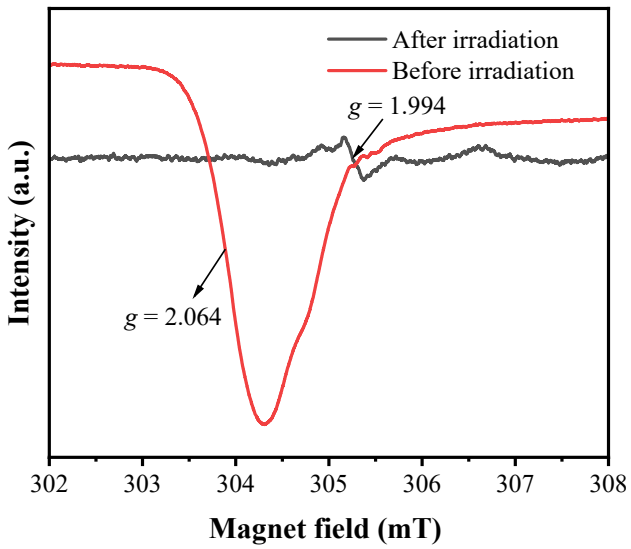

Fig. S8 EPR spectra of SA-Cu/TiO_2(B)-V_O adsorbed with Cu ions before and after photoreduction.

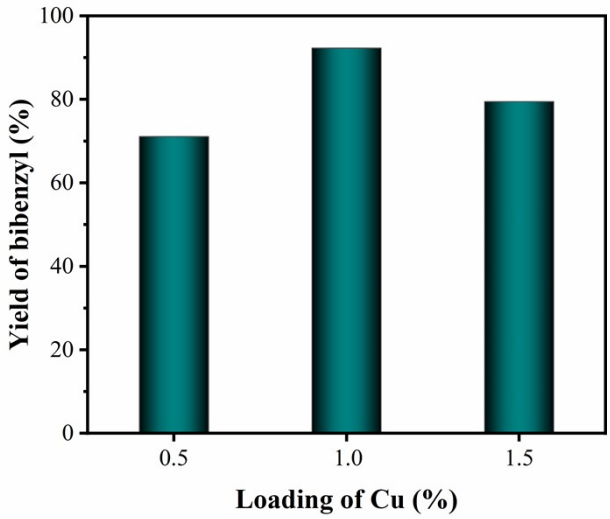

Fig. S9 The effect of Cu loading on photocatalytic synthesis of bibenzyl under irradiation

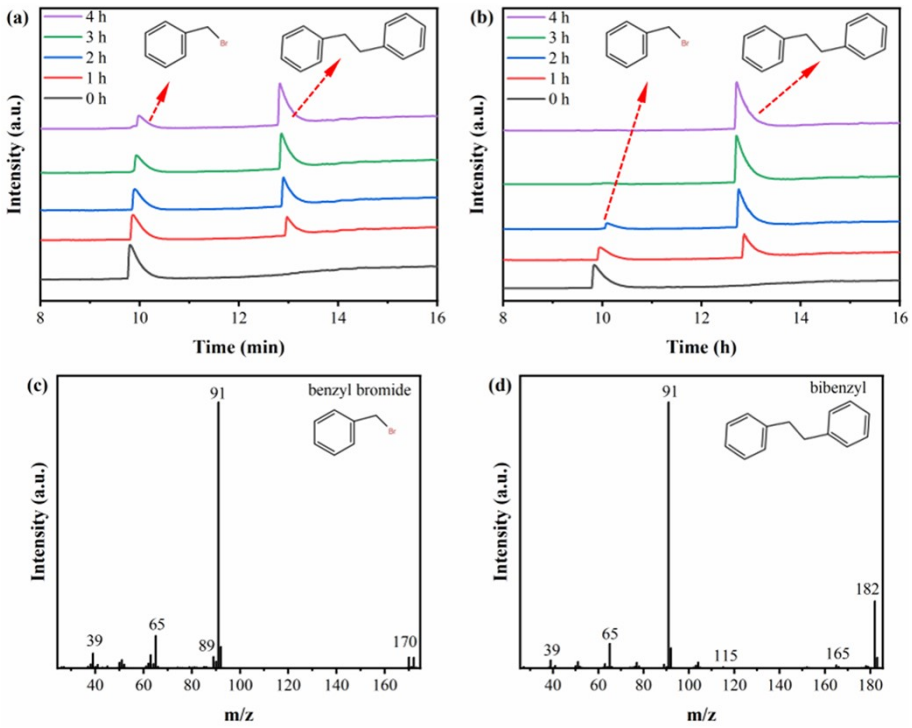

Fig. S10 (a-b) GC spectra at different reaction times in pure and aqueous isopropanol in the presence of SA-$Cu_{1.0}$/TiO_2(B)-V_O; (c) mass spectrum of the reactant, benzyl bromide; (d) mass spectrum of the product, bibenzyl

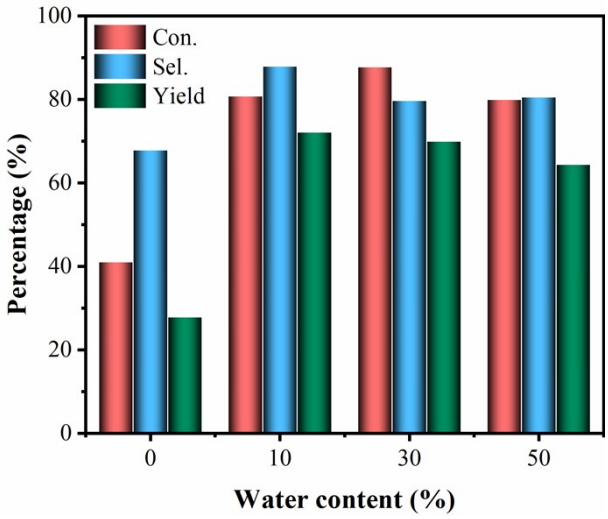

Fig. S11 The effect of water concentration on photocatalytic coupling synthesis of bibenzyl after irradiation of 2 h.

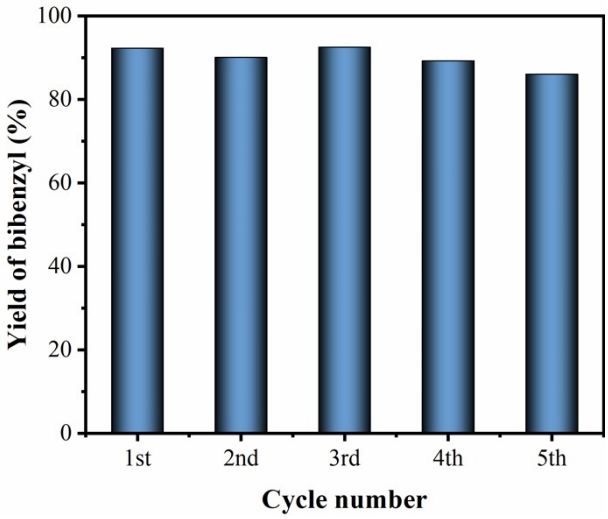

Fig. S12 The photocatalytic cycle tests for SA-$Cu_{1.0}$/TiO_2(B)-V_O.

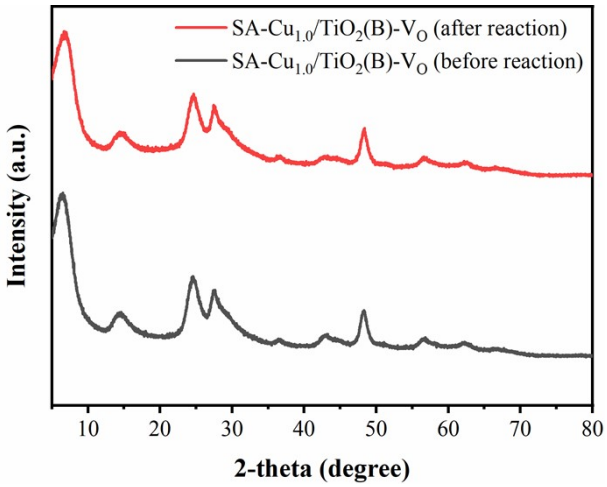

Fig. S13 XRD pattern of SA-$Cu_{1.0}$/TiO_2(B)-V_O before and after the photocatalytic reaction.

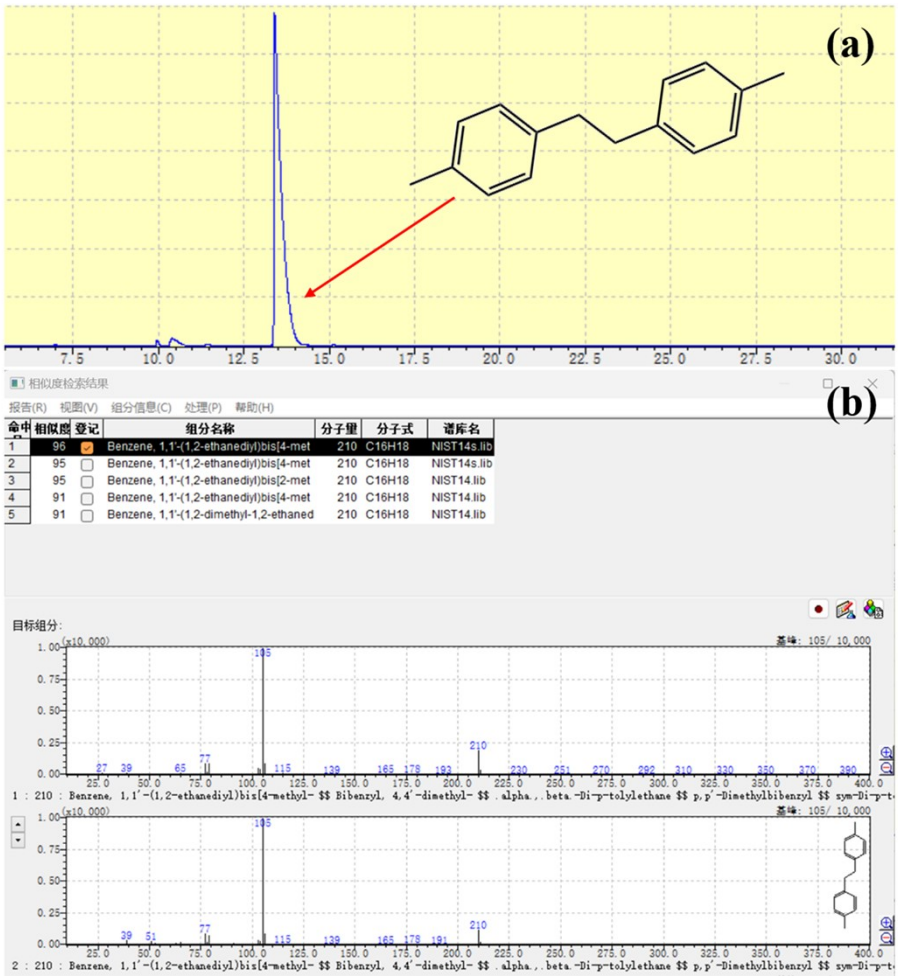

Fig. S14 4-methylbenzene bromide as substrate, (a) GC data. (b) MS data.

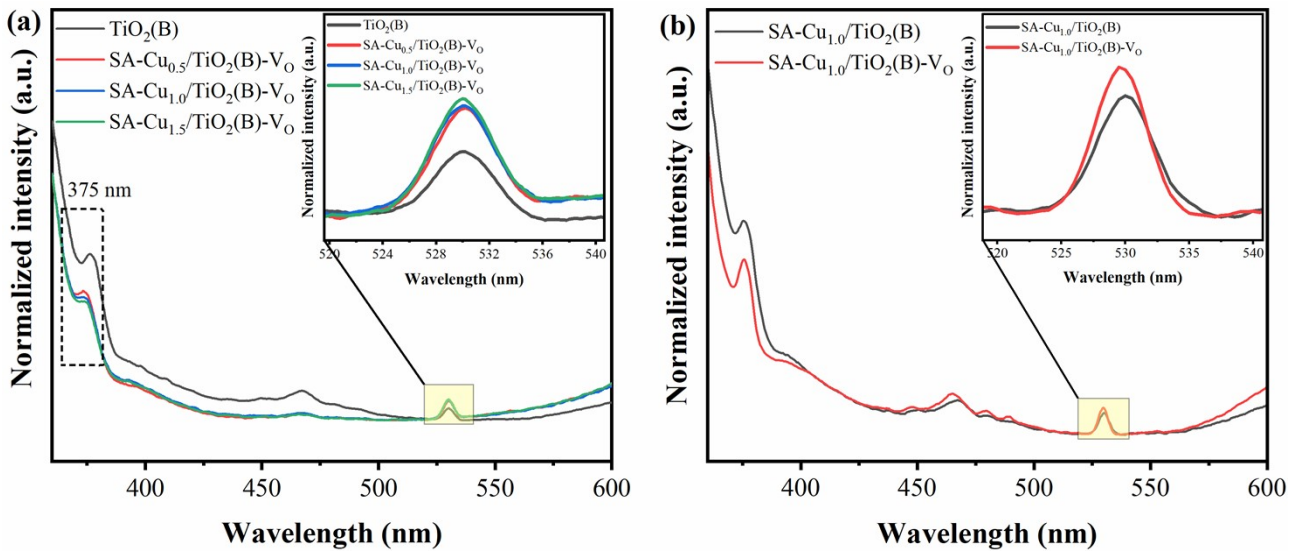

Fig. S15 (a) PL spectra of SA-Cu_x/TiO_2(B)-V_O photocatalysts. (b) PL spectra of SA-$Cu_{1.0}$/TiO_2(B)-V_O photocatalyst before and after air annealing.

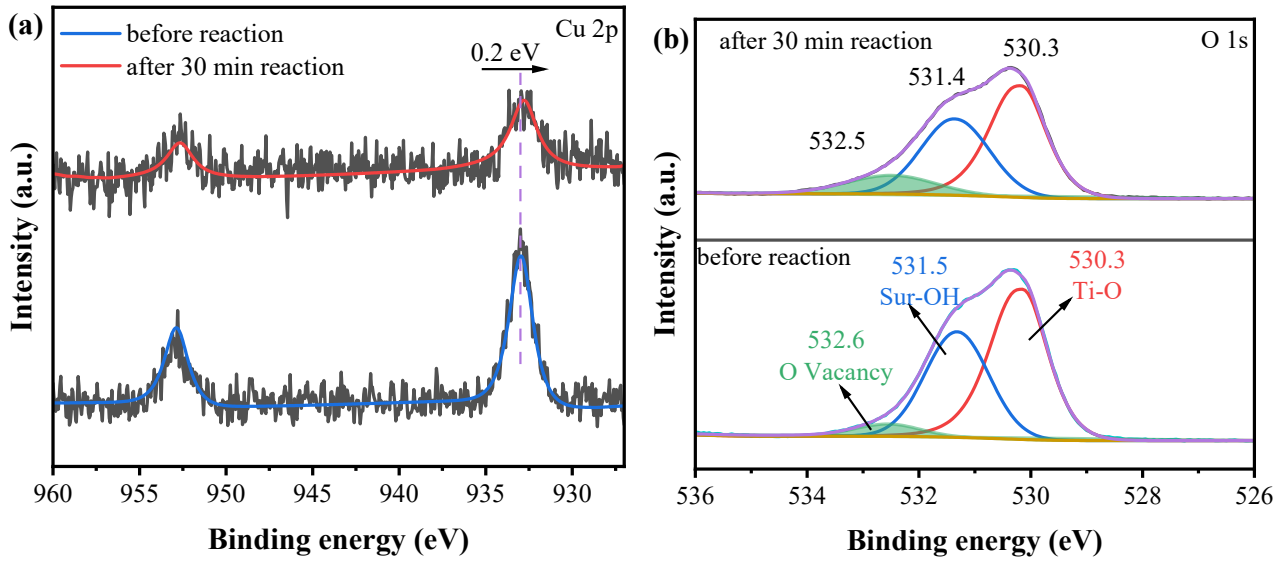

Fig. S16 XPS spectra of TiO_2(B) and SA-Cu1.0/TiO_2(B)-V_O photocatalyst before and after irradiation of 30 mins, Cu 2p (a) and O 1s (b).

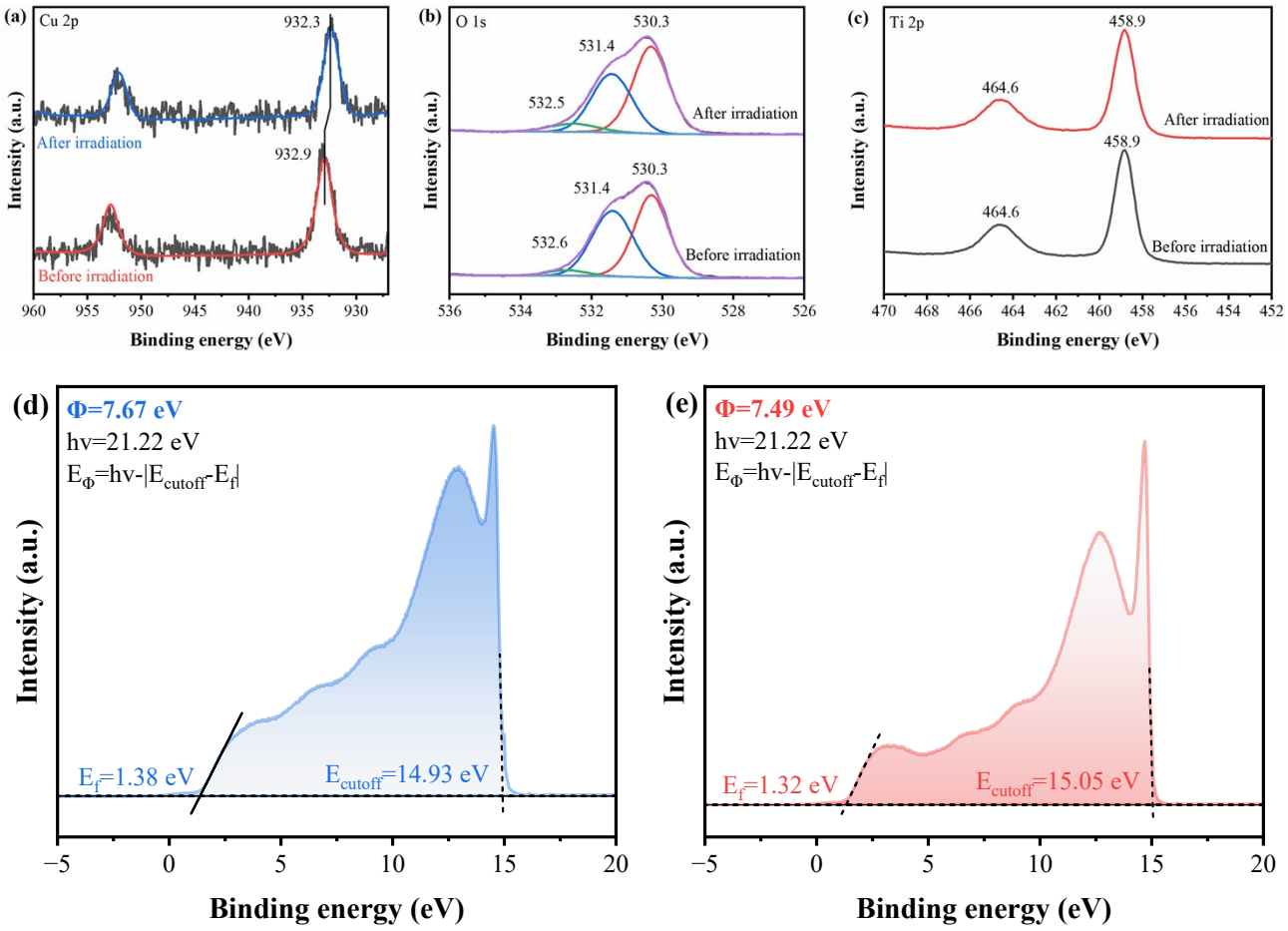

Fig. S17 XPS spectra of SA-$Cu_{1.0}$/TiO_2(B)-V_O photocatalyst before and after ireaction (a-c), and UPS spectra of TiO_2(B) and SA-$Cu_{1.0}$/TiO_2(B)-V_O (d-e).

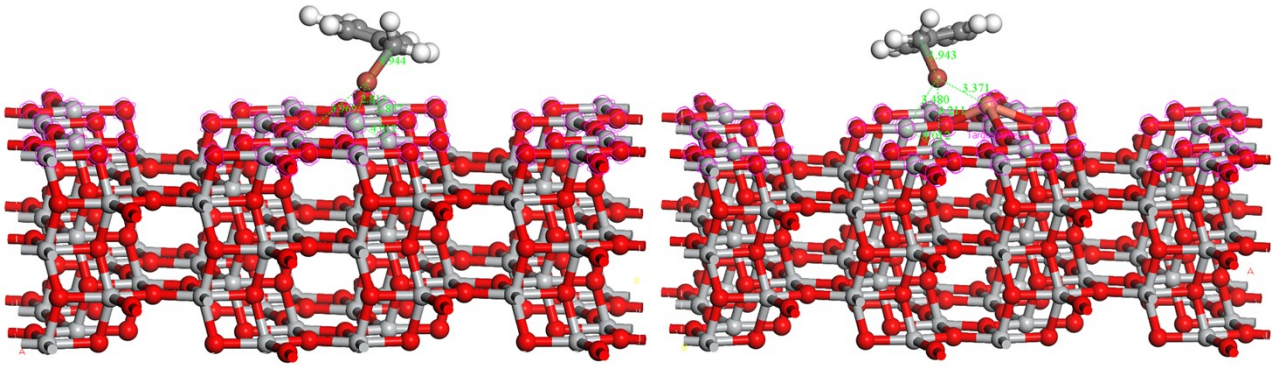

Fig. S18 Changes of C−Br bond length of benzyl bromide before and after introduction of single atom Cu.

Table S1 ICP-OES content analysis of Cu on the surface of SA-Cu_x/TiO_2(B)-V_O.

Sample	The theoretical loading	The actual loading
SA-$Cu_{0.5}/TiO_2$(B)-V_O	0.50%	0.43%
SA-$Cu_{1.0}/TiO_2$(B)-V_O	1.00%	0.83%
SA-$Cu_{1.5}/TiO_2$(B)-V_O	1.50%	1.14%

Table S2 Pore radius volume, and specific surface area of SA-Cu_x/TiO_2(B)-V_O photocatalysts.

Entry	Photocatalysts	Pore Volume (cm^3/g)	Pore semidiameter (Å)	BET surface area (m^2/g)
1	TiO_2(B)	0.89	64.2	279.4
2	SA-$Cu_{0.5}$/TiO_2(B)-V_O	0.62	41.1	301.7
3	SA-$Cu_{1.0}$/TiO_2(B)-V_O	0.75	52.9	285.6
4	SA-$Cu_{1.5}$/TiO_2(B)-V_O	0.58	40.3	288.9

Table S3 Atom percentages of O 1s peaks determined by the XPS analysis.

Sample	TiO_2(B)	SA-$Cu_{1.0}$/TiO_2(B)-V_O
O_1	530.3 (47.75%)	530.4 (50.33%)
O_2	531.4 (48.14%)	531.5 (38.39%)
O_3	532.9 (4.11%)	532.6 (11.28%)

Table S4 Adsorption capacity of different photocatalysts for substrate molecules.

Sample	Substrate added (g)	Solution weight (g)	Substrate content before adsorption	Substrate content after adsorption	Adsorption coefficient
$Cu^{2+}/TiO_2(B)\text{-}V_O$	0.02565	10.3023	0.002490	0.002477	0.005049
$TiO_2(B)\text{-}V_O$	0.0266	10.2199	0.002603	0.002600	0.000816
$Cu/TiO_2(B)\text{-}V_O$	0.0248	10.1862	0.002435	0.002385	0.020219
Cu^{2+}	0.0269	10.2357	0.002628	0.002618	0.003986

Table S5 Photocatalytic conversion of benzyl bromide in different solvents.

Entry	Solvent	Conversion (%)	Selectivity (%)	Yield (%)
1	Isopropanol	67.38	64	43.12
2	Ethanol	99.33	68.59	68.13
3	Methanol	100	91.59	91.59
4	Isopropanol solution (10 vol% water)	100	92.32	92.32
5	Ethanol solution (10 vol% water)	100	96.78	96.78
6	Methanol solution (10 vol% water)	100	97.20	97.20
7	Acetonitrile solution (30 vol% water)	57.65	74.83	43.14

Table S6 Adsorption energy of benzyl bromide and bibenzyl at different adsorption sites.

	E(A-B)/(kcal/mol)	EA (kcal/mol)	EB (kcal/mol)	Eint (kcal/mol)
PhBr@TiO_2(B)(010)	−193226.1222	−193209.4167	5.599547	−22.305034
PhBr@TiO_2(B)(010)V_O	−192366.4991	−192348.6626	5.600752	−23.437319
PhBr@TiO_2(B)(010)V_O+Cu	−67638.52796	−67601.91634	4.905675	−41.517295
BiPh@TiO_2(B)(010)V_O+Cu	−67651.62836	−67651.62836	1.086108	−1.086108
PhBr+BiPh@TiO_2(B)(010)+Cu	−68499.3117	−68499.3117	5.565367	−5.565367